J. Fluid Mech. (1986), *vol.* 171, *pp.* 477–494
Printed in Great Britain

Wavenumber selection in ramped Rayleigh–Bénard convection

By JEFFREY C. BUELL AND IVAN CATTON

Department of Mechanical, Aerospace and Nuclear Engineering, University of California, Los Angeles, CA 90024, USA

(Received 25 October 1985 and in revised form 21 April 1986)

We consider wavenumber selection for the periodic two-dimensional Rayleigh–Bénard problem on a horizontally infinite domain. The temperature difference (and hence the Rayleigh number) is assumed to be a slowly varying function of the horizontal coordinate perpendicular to the convection rolls. Under this condition Kramer *et al.* have shown that a unique wavenumber of convection is selected by a certain solvability condition if the domain contains a subcritical region. They performed analytic calculations for a model problem and for small-amplitude convection of an infinite-Prandtl-number fluid between stress-free boundaries. Their results are extended here to the realistic case of large-amplitude convection of a finite-Prandtl-number fluid between rigid boundaries. The temperature difference may be 'ramped' by changing either the temperature at the lower boundary or at the upper boundary, or both. It is shown that the choice has a significant effect on the 'mean flow', but no effect on the selected wavenumber.

1. Introduction

A well-known attribute of natural convection in a horizontally large domain is the possibility of many different linearly stable patterns. This fact hampers the numerical prediction of the field quantities and their various functionals (for example, heat transfer) because these will depend, in general, on the initial conditions. Furthermore, the numerical approximation must contain many degrees of freedom since the horizontal lengthscale of the container is much larger than that of an individual convection cell. In many cases computational requirements result that are not available or simply not practical. To overcome these difficulties, one usually assumes periodic solutions with some wavenumber, and then solves the governing equations over just one cell defined by the periodicity. This works well, but only if the wavenumber is specified in advance. For Rayleigh–Bénard convection, two-dimensional periodic rolls are stable (between the first and second bifurcation points) for all wavenumbers in a fairly large range. Thus, essentially the entire problem is reduced to finding an independent equation for the wavenumber.

Early efforts in the search for such an equation concentrated on selection criteria that would yield a 'preferred' wavenumber. It was assumed (at least implicitly) that this wavenumber depends only on the local physics and convection patterns. For instance, Malkus & Veronis (1958) suggested several criteria by which unique wavenumbers may be obtained. These included maximum heat transfer and maximum mean-squared temperature gradient, which were favoured as selection criteria for many years. Another possible criterion was given by Platzman (1965), who assumed the preferred wavenumber was defined by maximizing the temporal growth rate. All

of these criteria (along with several other proposals) overpredicted both the wavenumber and the heat transfer in comparison with experiments, and none addressed the relevant physics. A partially successful attempt to solve this problem more rigorously was made by McDonough (1980), who utilized the non-equilibrium thermodynamic theory of Glansdorff & Prigogine (1971). McDonough's work reproduced experimental wavenumbers, but it suffered from having to make a somewhat arbitrary assumption regarding the definition of a 'fluctuation', and from the need to use empirical data to define one of the parameters required by the theory.

Since about 1980, attention has turned towards selection mechanisms that take into account the global physics and geometry of particular systems, and which can be more fully justified. Thus, locally two-dimensional rolls may appear in many contexts, but there is no theoretical reason to expect the selected wavenumber to be the same in all of them. In typical experiments, convection is set up in a large-aspect-ratio container. Without control over the initial conditions, one observes a disorganized pattern of locally two-dimensional rolls. These patterns contain several possible wavenumber selection mechanisms such as roll curvature and dislocations (for example, see Cross & Newell 1984, and references therein), as well as the effect of the lateral boundaries. Individually, these effects are at least partially understood but very little progress has been made on understanding the interactions in the general problem. Consequently, what has been done recently, and what we intend to do here, is to examine one mechanism by itself. This yields results that are applicable only to the class of problems corresponding to the particular mechanism, but it should clarify the physics involved in a rigorous and non-empirical manner. We submit that this understanding is necessary before more difficult problems are attacked.

For instance, Manneville & Piquemal (1983), and Buell & Catton (1986), considered rolls that are slightly curved and far away from lateral boundaries. The first paper was for small-amplitude convection near the critical point and the second for finite-amplitude convection up to the onset of three-dimensional flow. They showed that for finite Prandtl numbers a net flow or a mean pressure gradient is generated perpendicular to the roll axis. A free parameter defines the magnitude of one of them and the type of flow that results. The two most common possibilities are (i) the net flow is zero, yielding axisymmetric convection, and (ii) the mean pressure gradient is zero, yielding the boundary of the zigzag instability. Since these effects are generated by the horizontal advection term of the momentum equation, wavenumber selection in axisymmetric convection and the zigzag instability are identical problems at infinite Prandtl number. This is probably the basis of some (incorrect) conjectures in the literature to the effect that the boundary of the zigzag instability is a selection criterion for finite Prandtl numbers. In both of the above cases, the governing equations and dependent variables are expanded in an asymptotic series with respect to the inverse of the radius of curvature. At zeroth order, the governing equations in Cartesian coordinates are recovered and are solved for the basic flowfields. Steady solutions at first order can only be obtained if a certain solvability condition, which depends on the above free parameter, is satisfied. Since the only other free parameter is the wavenumber, the solvability condition becomes the wavenumber selection criterion. Comparisons by Buell & Catton (1986) of the predicted wavenumber with axisymmetric experiments at many different Rayleigh and Prandtl numbers were all very good.

Another selection mechanism – one that should find applicability beyond convection problems – is described by Kramer *et al.* (1982). One (or more) of the original

(dimensional) parameters is 'ramped' slowly in the direction perpendicular to the roll axis so that the (non-dimensional) forcing parameter (for example, the Rayleigh number) increases slowly. The slow variation is quantified by introducing a small parameter ϵ, which is analogous to the inverse of the radius of curvature for the small-curvature problem. Again, the governing equations and dependent variables are expanded in terms of the small parameter, and a solvability condition is obtained. The difference here is that this condition contains the first derivative of the wavenumber with respect to the slow variable, thus an ordinary differential equation (ODE) for the selected wavenumber is obtained instead of an algebraic equation as above. If the slow variation is such that the system becomes critical at some point, then the ODE can be solved using the critical values as the initial condition. Kramer & Riecke (1985) applied these ideas to the stress-free, infinite Prandtl-number problem near the critical point by varying both the temperature difference and the plate gap, and found the initial slope of the selected wavenumber with respect to the Rayleigh number. One of their more interesting results was that the initial slope depends very strongly on which dimensional parameter was varied.

In this paper we extend Kramer & Riecke's analysis to the more physically realistic case of rigid plates and large-amplitude convection at finite Prandtl number, but consider only the case where the temperature difference is ramped. The resulting non-uniformity of the temperature boundary conditions forces a mean flow (averaged horizontal velocity) proportional to the slope of the ramp. A parameter is introduced that describes how the boundary conditions are varied in order to achieve the desired temperature difference, and it is shown that its value affects only the mean flow, but not the selection criterion. We emphasize that the variable-gap case does not present any conceptual difficulties, just algebraic ones; we are considering extending the analysis to this problem.

One of the main assumptions we make is the existence of two-dimensional transverse (that is, perpendicular to the gradient of the temperature difference) rolls. Intuitively, one would expect that longitudinal (parallel to the temperature difference gradient) rolls would be preferred since the mean flow creates a situation similar to convection with an imposed shear flow. However, determining the preferred mode is more complicated than this since the mean flow is much smaller than commonly encountered shear flows, and the effects of lateral boundary conditions and the initial condition may be just as important. Theoretical results related to the transverse-roll assumption are mixed. Walton (1982, 1983) analysed the stability of this problem near the critical point with free–free boundary conditions and various geometrical assumptions. He found that both transverse and longitudinal rolls can be expected, depending on the geometry and the lateral boundary conditions.

The quantity of experimental results is also limited. Convection in a cylindrical container with an imposed radial temperature gradient was studied by Koschmieder (1966). He observed axisymmetric convection (which corresponds to transverse rolls), but the effect of roll curvature is probably just as important as the non-uniform heating. A rectangular box of (non-dimensional) size 10:4:1 was used by Srulijes (1979) in the experiment that most closely parallels the work carried out here. He varied the temperature difference in the long dimension, but an aspect ratio of 10 is not large enough for quantitative comparisons. He observed fully three-dimensional flow and a bifurcation to longitudinal rolls for larger slopes of the temperature-difference ramp. It does not follow, however, that two-dimensional transverse rolls could not have been obtained if a slower ramp had been used or if different conditions on the temperature at the lateral boundaries had been imposed.

The theory presented here can also be applied to the other types of flow observed by Srulijes. If the transverse dimension of the container is not large, then the flow is necessarily three-dimensional and the corresponding conservation equations must be solved. The 'wavenumber equation' is the same except for additional terms arising from derivatives in the transverse direction. This will be the subject of a future investigation. The asymptotic analysis can also be carried out for longitudinal rolls, but in this case the wavenumber equation appears at second order, and a second-order ODE is obtained. An additional condition on the initial slope is needed to make the problem well posed, but it is not known what its value should be. Furthermore, dislocations will inevitably appear in the flow (possibly in a non-unique manner), which may well make the problem intractable.

In §2 we present the asymptotic analysis that leads to the wavenumber equation. A short review of the numerical method used to solve the governing equations is given in §3. Results for the selected wavenumber are discussed in §4, along with an analysis of the effects of the initial condition and the numerical approximation. A few final remarks are made in §5.

2. Wavenumber selection

In this section we derive the governing equations for the velocity and temperature fields, and give the asymptotic analysis which will yield the wavenumber selection criterion.

The partially scaled conservation equations for the horizontal and vertical velocities u and w, the temperature T, and the reduced pressure p are

$$u_x + w_z = 0, \tag{1a}$$

$$\frac{1}{P}u_t = \nabla^2 u - p_x - \frac{1}{P}(uu_x + wu_z), \tag{1b}$$

$$\frac{1}{P}w_t = \nabla^2 w - p_z + \frac{g\alpha}{\nu\kappa}D^3(T - T_0) - \frac{1}{P}(uw_x + ww_z), \tag{1c}$$

$$T_t = \nabla^2 T - uT_x - wT_z, \tag{1d}$$

where we used the Boussinesq approximation and scaled lengths with the layer height D, time with D^2/κ, and pressure with $\rho_0 \kappa\nu/D^2$. The Prandtl number is $P = \nu/\kappa$. Here, α is the coefficient of thermal expansion, g the acceleration due to gravity, ν the kinematic viscosity, κ the thermal diffusivity and ρ_0 the density at temperature T_0. Partial differentiation with respect to the horizontal and vertical coordinates, and time is denoted by the subscripts x, z, and t respectively. The two-dimensional Laplacian is

$$\nabla^2 = \frac{\partial^2}{\partial x^2} + \frac{\partial^2}{\partial z^2}.$$

The only dimensional unknown in (1) is the temperature, which is not as easily non-dimensionalized since we are allowing the temperature of the two plates to vary. The boundary conditions on T are

$$T = T_{\mathrm{H}}(x), \quad z = 0,$$

$$T = T_{\mathrm{C}}(x), \quad z = 1.$$

Let T_H and T_C be related to each other through the parameter z_0:

$$T_H = T_0 + z_0 \Delta T(x),$$
$$T_C = T_0 + (z_0 - 1)\Delta T(x),$$

where ΔT is the temperature difference $T_H - T_C$ and T_0 is the temperature at $z = z_0$ in the basic linear temperature profile, which implies that it is independent of x. We now define the slow variation of ΔT by setting

$$\Delta T = \Delta T_0(1 + \epsilon x), \quad \epsilon \ll 1, \tag{2}$$

where ΔT_0 is a reference quantity. A non-dimensional temperature θ is given by

$$T - T_0 = (\theta + z_0 - z)\Delta T_0(1 + \epsilon x). \tag{3}$$

We eliminate pressure and the continuity equation (1*a*) by substituting

$$u = \phi_{xz}, \quad w = -\phi_{xx}, \tag{4}$$

and taking the vertical component of the curl(curl) of the vector momentum equation (1*b*, *c*). A simpler two-dimensional stream function could have been used here, but the above is the restriction to two dimensions of the general three-dimensional solenoidal velocity field representation (Busse 1967) and therefore its use is advantageous from the point of view of code development. The resulting equations are

$$\frac{1}{P}\nabla^2\phi_{xxt} = \nabla^4\phi_{xx} - R\theta_{xx} - 2\epsilon R_0\theta_x - \frac{1}{P}\frac{\partial}{\partial x}(\phi_{xz}\nabla^2\phi_{xx} - \phi_{xx}\nabla^2\phi_{xz}), \tag{5a}$$

$$\theta_t = \nabla^2\theta - \phi_{xx} - \phi_{xz}\theta_x + \phi_{xx}\theta_z + \frac{R_0}{R}\epsilon(2\theta_x - \phi_{xz}(\theta + z_0 - z)), \tag{5b}$$

where R is the local Rayleigh number

$$R = \frac{\alpha g D^3 \Delta T}{\nu\kappa},$$

and R_0 is the Rayleigh number based on ΔT_0. If we make the no-slip and infinite-conductivity-plates assumptions, the boundary conditions are

$$\phi = \phi_z = \theta = 0, \quad z = 0, 1. \tag{6}$$

An examination of (5) shows that the solutions will depend on two horizontal lengthscales. This suggests performing a multiple-scale analysis by replacing x with a 'fast' variable η and a 'slow' variable $X = \epsilon x$. Following Kramer *et al.* (1982), we define a phase variable σ by $R_0\sigma(X, \tau) = \epsilon\eta$, where the corresponding slow timescale is $\tau = \epsilon^2 t$. Assuming that the wavenumber a varies slowly and the field variables are 2π-periodic in η, we have

$$\frac{\partial\eta}{\partial x} = \frac{\partial\sigma}{\partial X} = a(X). \tag{7}$$

This implies that

$$\frac{\partial}{\partial x} = a(X)\frac{\partial}{\partial\eta} + \epsilon\frac{\partial}{\partial X}. \tag{8}$$

Since R depends only on X, we see that it may be convenient to replace X with R as follows:

$$\frac{\partial}{\partial x} = a(R)\frac{\partial}{\partial\eta} + \epsilon R_0\frac{\mathrm{d}}{\mathrm{d}R}. \tag{9a}$$

The total derivative was used here because we can also write

$$\frac{\partial}{\partial X} = R_0 \frac{\partial}{\partial R} + R_0 \frac{\mathrm{d}a}{\mathrm{d}R} \frac{\partial}{\partial a}.$$

This was used in the analytical work of Kramer *et al.* (1982) and Kramer & Riecke (1985), but for numerical calculations (9*a*) is much more efficient. One must, however, be careful in its implementation: higher derivatives with respect to x are found using the chain rule on (8), and then reformulating as in (9*a*). Expanding the derivatives in this manner yields

$$\frac{\partial^2}{\partial x^2} = a^2 \frac{\partial^2}{\partial \eta^2} + \epsilon R_0 \left(\frac{\mathrm{d}a}{\mathrm{d}R} \frac{\partial}{\partial \eta} + 2a \frac{\mathrm{d}}{\mathrm{d}R} \frac{\partial}{\partial \eta} \right) + \ldots, \tag{9b}$$

$$\frac{\partial^3}{\partial x^3} = a^3 \frac{\partial^3}{\partial \eta^3} + \epsilon R_0 \left(3a \frac{\mathrm{d}a}{\mathrm{d}R} \frac{\partial^2}{\partial \eta^2} + 3a^2 \frac{\mathrm{d}}{\mathrm{d}R} \frac{\partial^2}{\partial \eta^2} \right) + \ldots, \tag{9c}$$

$$\frac{\partial^4}{\partial x^4} = a^4 \frac{\partial^4}{\partial \eta^4} + \epsilon R_0 \left(6a^2 \frac{\mathrm{d}a}{\mathrm{d}R} \frac{\partial^3}{\partial \eta^3} + 4a^3 \frac{\mathrm{d}}{\mathrm{d}R} \frac{\partial^3}{\partial \eta^3} \right) + \ldots, \tag{9d}$$

$$\frac{\partial^5}{\partial x^5} = a^5 \frac{\partial^5}{\partial \eta^5} + \epsilon R_0 \left(10a^3 \frac{\mathrm{d}a}{\mathrm{d}R} \frac{\partial^4}{\partial \eta^4} + 5a^4 \frac{\mathrm{d}}{\mathrm{d}R} \frac{\partial^4}{\partial \eta^4} \right) + \ldots, \tag{9e}$$

$$\frac{\partial^6}{\partial x^6} = a^6 \frac{\partial^6}{\partial \eta^6} + \epsilon R_0 \left(15a^4 \frac{\mathrm{d}a}{\mathrm{d}R} \frac{\partial^5}{\partial \eta^5} + 6a^5 \frac{\mathrm{d}}{\mathrm{d}R} \frac{\partial^5}{\partial \eta^5} \right) + \ldots, \tag{9f}$$

where implicit dependence of a on R is assumed. The time derivative becomes

$$\frac{\partial}{\partial t} = \epsilon R_0 \frac{\partial \sigma}{\partial \tau} \frac{\partial}{\partial \eta}. \tag{10}$$

We can write the field variables in a similar asymptotic form (suppressing the explicit dependencies on the vertical coordinate and time),

$$\phi(x) = \phi^{(0)}(\eta, X) + \epsilon R_0 \phi^{(1)}(\eta, X) + \ldots, \tag{11a}$$

$$\theta(x) = \theta^{(0)}(\eta, X) + \epsilon R_0 \theta^{(1)}(\eta, X) + \ldots. \tag{11b}$$

Substituting (9), (10), and (11) into (5), the governing equations at each order in ϵ can be derived. Since ϵ always appears multiplied by R_0, we set $R_0 = 1$ with no loss of generality. Also, it is convenient to set $a(\partial/\partial\eta) = \partial/\partial x$ (of course, this can be done only after the equations are developed). At order ϵ^0, we have the Boussinesq equations:

$$\nabla^4 \phi^{(0)}_{xx} - R\theta^{(0)}_{xx} - \frac{1}{P} \frac{\partial}{\partial x} (\phi^{(0)}_{xz} \nabla^2 \phi^{(0)}_{xx} - \phi^{(0)}_{xx} \nabla^2 \phi^{(0)}_{xz}) = 0, \tag{12a}$$

$$\nabla^2 \theta^{(0)} - \phi^{(0)}_{xx} - \phi^{(0)}_{xz} \theta^{(0)}_x + \phi^{(0)}_{xx} \theta^{(0)}_z = 0. \tag{12b}$$

This system determines the periodic solutions corresponding to the local value of R, but the wavenumber remains undetermined. Before the equations at order ϵ^1 are given, we note that the non-uniformity of the temperature boundary conditions will create a horizontal mean flow for both subcritical and supercritical Rayleigh numbers. However, a mean flow cannot be contained in the ansatz (4), so we will need a separate equation for it. This is obtained by substituting (3), (9), and (11) into (1*b*, *c*), eliminating the pressure between (1*b*) and (1*c*), and then horizontally averaging the

result. The mean flow corresponding to the series (11*a*) is denoted by $\epsilon\overline{u}(z)$. Noting that the time derivatives are identically zero at this order, the resulting equation is

$$\overline{u}_{zzz} = \langle\theta^{(0)} + R\theta_R^{(0)}\rangle + z_0 - z + \frac{1}{P}\frac{\partial}{\partial z}\Big\langle \frac{1}{a}\frac{\mathrm{d}a}{\mathrm{d}R}[(\phi_{xz}^{(0)})^2 - 4(\phi_{xx}^{(0)})^2 - \phi_x^{(0)}\phi_{xzz}^{(0)}]$$
$$-\phi_{xxz}^{(0)}\phi_{zR}^{(0)} - \phi_{xx}^{(0)}\phi_{zzR}^{(0)} + 2\phi_{zz}^{(0)}\phi_{xxR}^{(0)} - 2\phi_{xx}^{(0)}\phi_{xxR}^{(0)} - \phi_{xx}^{(0)}\phi_{xzz}^{(1)} - \phi_{xzz}^{(0)}\phi_{xx}^{(1)}\Big\rangle, \quad (13)$$

where the angled brackets denote the horizontal average over a wavelength. Integrating once yields

$$\overline{u}_{zz} = \int_0^z \langle\theta^{(0)} + R\theta_R^{(0)}\rangle\,\mathrm{d}\xi + z(z_0 - \tfrac{1}{2}z)$$
$$+\frac{1}{P}\Big\langle \frac{1}{a}\frac{\mathrm{d}a}{\mathrm{d}R}[(\phi_{xz}^{(0)})^2 - 4(\phi_{xx}^{(0)})^2 - \phi_x^{(0)}\phi_{xzz}^{(0)}] - \phi_{xxz}^{(0)}\phi_{zR}^{(0)} - \phi_{xx}^{(0)}\phi_{zzR}^{(0)}$$
$$+2\phi_{zz}^{(0)}\phi_{xxR}^{(0)} - 2\phi_{xx}^{(0)}\phi_{xxR}^{(0)} - \phi_{xx}^{(0)}\phi_{xzz}^{(1)} - \phi_{xzz}^{(0)}\phi_{xx}^{(1)}\Big\rangle + \overline{p}, \quad (14)$$

where $\overline{p}$ is the constant of integration, which contains the mean horizontal pressure gradient. The mean flow must also satisfy the no-slip boundary conditions: $\overline{u}(0) = \overline{u}(1) = 0$. The specific problem (or class of problems) determines $\overline{p}$. However, the most common physical situation is convection in a finite container with non-porous lateral walls. Thus, $\overline{p}$ is detemined by requiring the net flow,

$$\int_0^1 \overline{u}(z)\,\mathrm{d}z,$$

to be zero. The easiest way to do this is to first let $\overline{v}$ be the solution to (14) with $\overline{p} = 0$, so that

$$\overline{u} = \overline{v} + \overline{p}\tfrac{1}{2}z(z-1). \quad (15a)$$

The constant $\overline{p}$ is then determined by global conservation of mass, which yields

$$\overline{p} = 12\int_0^1 \overline{v}(z)\,\mathrm{d}z. \quad (15b)$$

Referring to (13), we note that the term $\langle\theta^{(0)} + R\theta_R^{(0)}\rangle$ is everywhere of the opposite sign as the odd component of $z_0 - z$. In addition it turns out that the former is slightly larger in magnitude than the latter, so that the two terms nearly cancel. The even part of the forcing is not affected by convection since it is completely contained within the term $z_0 - z$. (Here, 'odd' and 'even' refer to the parity of a function with respect to the mid-plane, $z = \frac{1}{2}$.) The terms multiplied by $1/P$ have the same parity as the temperature terms, but are considerably smaller.

After multiplying through by the wavenumber, the equations at order ϵ^1 can be written in the form

$$\frac{\partial\sigma}{\partial\tau}\left(\frac{1}{P}\nabla^2\phi_{xx}^{(0)}, \theta_x^{(0)}\right)^{\mathrm{T}} = \mathbf{M}[\boldsymbol{U}^{(0)}] + a\mathbf{L}[\boldsymbol{U}^{(1)}], \quad (16)$$

where $\boldsymbol{U}^{(i)} = (\phi^{(i)}, \theta^{(i)})^{\mathrm{T}}$, and a superscript T denotes the transpose. $\mathbf{M}$ is a nonlinear vector operator and $\mathbf{L}$ is the matrix operator obtained by linearizing (12) around $\boldsymbol{U}^{(0)}$. The elements of $\mathbf{M}$ and $\mathbf{L}$ are written out in the Appendix. Steady solutions exist only if the right-hand side of (16) vanishes. That is, $\boldsymbol{U}^{(1)}$ must satisfy

$$\mathbf{L}[\boldsymbol{U}^{(1)}] = -\frac{1}{a}\mathbf{M}[\boldsymbol{U}^{(0)}]. \quad (17)$$

A periodic solution for $U^{(1)}$ exists only if the solvability condition

$$(U^*, \mathbf{M}[U^{(0)}]) = 0, \tag{18}$$

is fulfilled, where U^* belongs to the null space of the adjoint of $\mathbf{L}$:

$$\mathbf{L}^*[U^*] = 0. \tag{19}$$

The adjoint is defined by

$$(V, \mathbf{L}[W]) = (\mathbf{L}^*[V], W),$$

where V and W are arbitrary functions satisfying the boundary conditions, and the inner product is the same as the one in (18). Here, we use the natural inner product for functions defined in Cartesian coordinates,

$$(V, W) = \int_0^1 \langle V \cdot W \rangle \, \mathrm{d}z.$$

The elements of the adjoint operator $\mathbf{L}^*$ are given in the Appendix. Equation (18) constitutes our selection criterion since the wavenumber (and its derivative) is the only quantity that can be varied so that the solvability condition is satisfied. Writing it as a first-order differential equation for the wavenumber, we have

$$F[a, U^*, U^{(0)}]\frac{\mathrm{d}a}{\mathrm{d}R} + G[a, U^*, U^{(0)}, \bar{u}]\, a = 0, \tag{20}$$

where the functionals F and G follow directly from (18) and (A 1). As an aside, we note that if the phase is unsteady and U^* is properly normalized, the above can be written

$$\frac{\partial \sigma}{\partial \tau} = F\frac{\partial^2 \sigma}{\partial X^2} + G\frac{\partial \sigma}{\partial X}. \tag{21}$$

Thus, the phase behaves diffusively with a 'longitudinal' diffusion coefficient F (Kramer *et al.* 1982) and convection (or 'drift') velocity $-G$. The former quantity is a property of the rolls while the latter contains all the information about the inhomogeneity (variable temperature, gap, etc.).

A single initial condition is needed to make (20) well posed. Usually, we take the values at the critical point:

$$a = a_c, \quad R = R_c, \tag{22}$$

where

$$a_c = 3.11632, \quad R_c = 1707.762,$$

but in general we simply have $a = a^0$, $R = R^0$. The wavenumber equation (20) is solved by an implicit mid-point scheme. All variables are defined on a discrete mesh in Rayleigh number space,

$$R^n = R^0 + n\Delta R,$$

where n (not necessarily an integer) is the step number and ΔR is the step size. At the nth step, derivatives with respect to R are evaluated with centred differences with respect to step $n-\frac{1}{2}$, for example,

$$\frac{\mathrm{d}a}{\mathrm{d}R} \approx \frac{a^n - a^{n-1}}{\Delta R}. \tag{23}$$

All other quantities are evaluated at the mid-point: $(R^{n-\frac{1}{2}}, a^{n-\frac{1}{2}})$, where $a^{n-\frac{1}{2}}$ is defined as $\frac{1}{2}(a^n + a^{n-1})$. Thus, at each step (20) becomes a nonlinear algebraic equation for a^n, which is iteratively solved by the fixed-point or the secant method until the

difference between two consecutive iterations is less than a given tolerance δ'. Because of the centred nature of all approximations, we expect that the predicted wavenumber will be second-order accurate in ΔR.

We summarize the above in the form of an algorithm for determining the selected wavenumber as a function of the Rayleigh number:

1. Input R^0, a^0, z_0, and the numerical parameters.
2. Solve for $U^{(0)}(R^0, a^0)$ and set $n = 0$.
3. Set $n = n+1$, $k = 0$, and guess (or extrapolate from lower n) a_0^n, where the subscript is the iteration counter.
4. Solve for $U^{(0)}(R^{n-\frac{1}{2}}, a_k^{n-\frac{1}{2}})$, $U^{(0)}(R^n, a_k^n)$, $U^*(R^{n-\frac{1}{2}}, a_k^{n-\frac{1}{2}})$, $\bar{u}$, and $U^{(1)}(R^{n-\frac{1}{2}}, a_k^{n-\frac{1}{2}})$, where the adjoint solution is based on the first solution, and the mean flow and perturbation solutions depend on the first two plus $U^{(0)}(R^{n-1}, a^{n-1})$. Also, if P is finite, $\bar{u}$ and $U^{(1)}$ are coupled and must be solved together, otherwise $U^{(1)}$ is not needed at all.
5. Evaluate the residual $r_k = F_k(a_k^n - a^{n-1})/\Delta R + G_k a_k^{n-\frac{1}{2}}$ of (20), and calculate a_{k+1}^n using
   (*a*) the fixed-point method for $k = 0$: $a_1^n = a^{n-1} - \Delta R a_0^{n-\frac{1}{2}} G_0/F_0$,
   (*b*) the secant method for $k > 0$: $a_{k+1}^n = a_k^n - r_k(a_k^n - a_{k-1}^n)/(r_k - r_{k-1})$.
6. If $|a_{k+1}^n - a_k^n| > \delta' \Delta R$, set $k = k+1$ and repeat steps 4 and 5.
7. Set $a^n = a_{k+1}^n$.
8. Repeat steps 3 to 7 until desired Rayleigh number is reached.

This procedure is straightforward and numerically well behaved. The exception is near the critical point, where there are terms in the functional G (such as $\mathrm{d}U^{(0)}/\mathrm{d}R$) that are $O((R/R_c - 1)^{-\frac{1}{2}})$ or $O(1)$. Since F is $O((R/R_c - 1)^{\frac{1}{2}})$, one would conclude that (20) is singular. However, given exact solutions these 'large' terms cancel out, leaving a well-posed problem (see Kramer & Riecke 1985 for an analysis of the free–free case). This is not quite true for the numerical work here; the large terms multiplied by the discretization error for the R derivatives do not cancel, but leave an error term that is of the same order of magnitude as F. Thus everything is finite, but an $O(1)$ error is introduced (only) at the first step if the critical values are used as the initial condition. To overcome this, we start the calculations one or two steps above the critical point and choose the initial condition so that a 'backward' extrapolation goes through the critical point. This starting procedure works quite well, and it will be shown later that the results at higher R are insensitive to the small errors caused by it.

On the other hand, the asymptotic expansions used here are non-uniform as R approaches the critical point (a different expansion is needed because $\bar{u}$ remains finite while $U^{(0)}$ goes to zero). Therefore, the wavenumber equation (20) may not be valid at the critical point even though it is non-singular. Starting at any supercritical R obviates this difficulty since a sufficiently small ϵ can always be found to make the expansions uniform.

3. Solution of the governing equations

Because of the requirement of speed and accuracy, it is worthwhile to review the numerical method used to solve the governing equations (12), (14), (17) and (19). The approach is the same as used by Buell & Catton (1986) and is similar to the methods used by McDonough & Catton (1982) for the Rayleigh–Bénard problem and by Meyer-Spasche & Keller (1978, 1980) for the rotating Taylor–Couette problem. All are mixed finite-difference Galerkin procedures where the Galerkin method is applied

in the horizontal (periodic) direction and finite differencing in the vertical (non-periodic) direction. We improve on the latter methods by implementing compact fourth-order accurate finite-difference schemes instead of standard centred second-order accurate differencing. Details of the method and most of the numerical analytic tests will be given elsewhere.

To illustrate the method, we apply it to (12). Suppressing superscripts, the solution is approximated by

$$\phi \approx \sum_{i=1}^{K} \phi_i(z) \cos a_i x, \tag{24a}$$

$$\theta \approx \sum_{i=0}^{K} \theta_i(z) \cos a_i x, \tag{24b}$$

where $a_i = ia$ and the boundary conditions on all of the ϕ_i, θ_i are the same as on ϕ, θ. Here we take advantage of the periodicity and symmetry properties of the solution (Clever & Busse 1974) in selecting the $\cos a_i x$ dependencies, while finite-difference methods are more suitable for the non-periodic boundary conditions on the upper and lower surfaces. Equations (24a) and (24b) are substituted into (12) and the Galerkin method applied in the horizontal direction only: we multiply by $\cos a_k x$ and integrate over a wavelength. Newton's method is applied next, but only with respect to ϕ_k and θ_k. Compared to a 'full' Newton's method, this reduces the amount of linear algebra that needs to be done by at least two orders of magnitude. Unfortunately, it also reduces the expected order of convergence of the iterations from quadratic to linear. It turns out (Buell & Catton 1986) that the former effect dominates the latter so that a large saving in computer time (as well as storage) is obtained.

The above procedure yields a coupled system of $2K+1$ ordinary differential equations for the modal functions ϕ_i and θ_i. These are solved one at a time by operator compact implicit (OCI) finite differencing on a uniform grid $z_j = h(j-1), j = 1,\ldots,J, h = 1/(J-1)$, where J is the number of grid points. OCI formulae are given by Stepleman (1976) for general second-order equations (here, these originate from (12b)), and by Buell (1986) for fourth-order equations (originating from (12a)). Both are fourth-order accurate with respect to the mesh spacing h, as compared to second-order accuracy for centred differencing.

Convergence tests demonstrating the accuracy of the numerical solution of (12) are given by Buell & Catton (1986). The modifications to the method necessary for the solution of the perturbation equations (17) and the adjoint equations (19) are also discussed. Convergence of the selected wavenumber with respect to the numerical parameters is demonstrated in the next section since the absolute accuracy of the calculated wavenumber cannot be predicted from the accuracy of the field solutions.

4. Results and discussion

In this section we shall present the main contribution of this work: the selected wavenumber as a function of the Rayleigh and Prandtl numbers. But first we show that the parameter z_0 does not affect the wavenumber. From (14) we see that the difference between $\bar{u}$ with $z_0 \neq \frac{1}{2}$, and $\bar{u}$ with $z_0 = \frac{1}{2}$ is

$$\bar{u}(z, z_0) - \bar{u}(z, \tfrac{1}{2}) = \tfrac{1}{6}(z_0 - \tfrac{1}{2})\, z(z-\tfrac{1}{2})(z-1), \tag{25}$$

which is an odd function and independent of convection. Typical terms that include $\overline{u}$ in the functional G are proportional to

$$\int_0^1 \theta_i^* \theta_i \overline{u}\,\mathrm{d}z, \quad \text{or} \int_0^1 \phi_i^* \phi_i \overline{u}\,\mathrm{d}z, \tag{26}$$

plus others that include the second derivative (which does not change the parity) of ϕ_i or $\overline{u}$. One finds from examining the forms of (12) and (A 3) that the modal functions U_i and U_i^* have the same parity and therefore the functions multiplying $\overline{u}$ are always even. It follows that the odd component of $\overline{u}$ does not contribute to integrals like the ones in (26) or (20). The only other place that z_0 appears is in the term $z_0 - z$ in (A 1*b*) which multiplies an odd function and, again, z_0 does not affect G. In performing the computations that follow we used $z_0 = \frac{1}{2}$, unless otherwise noted.

We mentioned earlier a special starting procedure that is needed to solve (20) so that large errors are avoided. In order to implement it, we require $a^0(R^0)$ for some R^0 slightly greater than R_c. Thus the initial slope of a with respect to R (denoted by a') must be determined. An estimate of this slope is obtained by selecting (iteratively) a^0 such that the equality in

$$a' \approx \frac{a^0 - a_c}{R^0 - R_c} = \frac{a^1 - a^0}{\Delta R} \tag{27}$$

is satisfied. The accuracy of this expression is determined by reducing R^0 and ΔR systematically. Considerable effort can be saved by taking ΔR to be $O((R^0 - R_c)^2)$, which replaces two independent sequences with one. Note that it is not sufficient for ΔR to be proportional to $R^0 - R_c$ because in this case the errors in the R derivatives of $U^{(0)}$ may become $O(1)$. The numerical parameters used were $J = 37$, $K = 4$, $\delta = 10^{-8}$, and $\delta' = 10^{-6}$. Additional tests ensured that the errors in the approximations these parameters represent are much smaller than the errors in (27). The extrapolation of $a'(R^0)$ to $R^0 = R_c$ gives a more accurate estimate of a', and it shows that the convergence rate of this procedure is greater than the linear rate one would expect. In table 1 extrapolated values of a' are given for several Prandtl numbers. Clearly, a' decreases monotonically with increasing P, as opposed to axisymmetric convection where a' decreases then increases slightly with P. These values are useful beyond their employment in (27); a' is accessible at the critical point to analytic calculations (similar to those by Manneville & Piquemal 1983 for the axisymmetric case) and so a valuable comparison is possible. Each number in the tables presented here is accurate up to the penultimate significant figure shown. The last figure is an estimate, the accuracy of which can only be determined by more extensive tests.

We now consider the numerical error in solving the wavenumber equation up to 'large' Rayleigh numbers. The convergence behaviour of the functionals F and G (and thus the wavenumber) with respect to the numerical parameters J, K, and δ is very similar to that of the Nusselt number (Buell & Catton 1986). Therefore, only an abridged version of these tests is given in table 2 from which the absolute accuracy of the calculated wavenumbers can be ascertained. Here, we integrated (20) up to $R = 12000$ starting from $R^0 = 3000$, $a^0 = 3.0448$, and using $P = 7.0$ and $\Delta R = 500$. Iteration tolerances for all large R calculations were $\delta = \delta' = 10^{-4}$, or smaller. The initial condition was obtained by performing the same procedure but starting just above R_c. It is apparent that the numerical error in the calculation of the wavenumber is very small. Less obvious is the effect of ΔR on the calculated wavenumber. Table 3 presents results for the same problem at several Rayleigh

P	0.025	0.3	0.5	0.7	1.0	1.5	3.0	7.0	∞
$a' \times 10^5$	485.0	33.3	12.2	5.54	1.62	−0.76	−2.55	−3.30	−3.74

TABLE 1. Initial slope a' as a function of the Prandtl number.

J	K	a
9	5	2.4462
13	9	2.4385
19	13	2.4402

TABLE 2. The selected wavenumber at $R = 12000$ as a function of number of grid points and modes. $P = 7$, $R^0 = 3000$, $a^0 = 3.0448$, $\Delta R = 500$.

R	$\Delta R = 1000$	$\Delta R = 500$	$\Delta R = 250$
6000	2.8040	2.8054	2.8058
9000	2.5972	2.5991	2.5996
12000	2.4368	2.4385	2.4389

TABLE 3. Convergence of the selected wavenumber with Rayleigh number step size. $P = 7$, $J = 13$, $K = 9$, $R^0 = 3000$, $a^0 = 3.0448$.

numbers for different values of ΔR with $J = 13$ and $K = 9$. We see that, as expected, the error is approximately second order in ΔR. In addition, the absolute error is quite small and is essentially independent of R. The latter observation means that errors do not accumulate with each step, which is an unusual property of a numerical solution of an initial-value problem.

This behaviour is at least partially explained by figure 1, where the selected wavenumber for $P = \infty$ is plotted using several different initial conditions. The middle line is for the case when the initial condition is the critical point. The converging nature of the solutions indicates that errors due to numerical approximations or errors in the initial condition tend to be damped. This figure also shows that if the system does not become critical at any point, then a unique wavenumber will not necessarily be selected. However, the band of allowable wavenumbers at high R will be small compared to the band of stable wavenumbers corresponding to the lowest Rayleigh number in the system. For instance, we see that a given band of wavenumbers at $R = 3000$ 'maps' to one about 17 times smaller at $R = 12000$.

The selected wavenumber as a function of the Rayleigh and Prandtl numbers is shown in figure 2. The qualitative behaviour of the initial slope of the wavenumber is reproduced at higher Rayleigh numbers in that the wavenumber is a monotonic decreasing function of P for all R. This function depends weakly on P when $P > 3$, but is sensitive to P when $P < 3$. The same dependence was also seen for wavenumber selection in axisymmetric convection (Buell & Catton 1986), and in fact the results are similar for the two cases (but not quite the same, differences are on the order of 0.2). There are no experiments based on using a variable temperature difference to measure wavenumbers known to the authors. As mentioned earlier, the experiments of Srulijes are the best available, but the aspect ratio he used (10) was not large

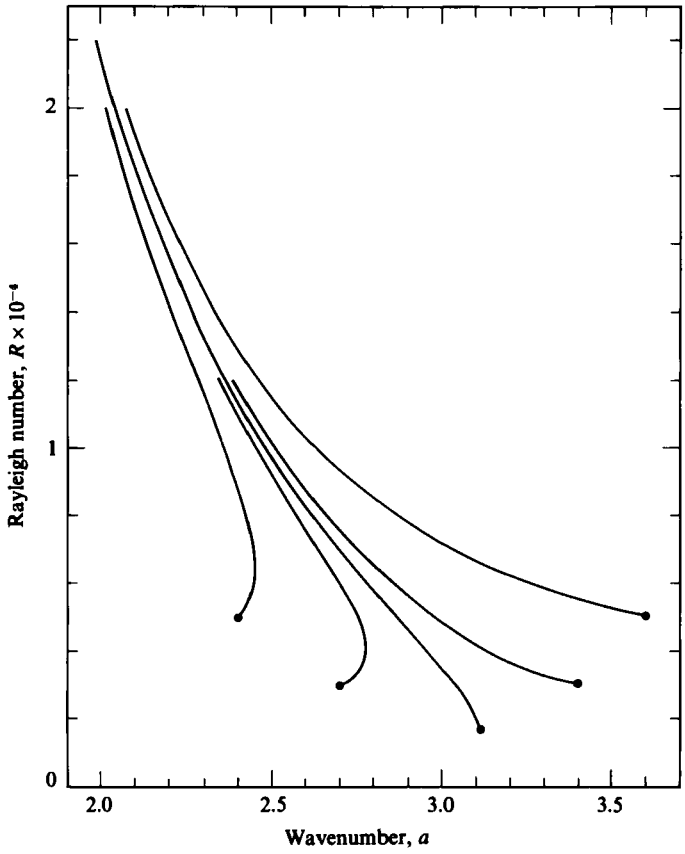

FIGURE 1. Solution of the wavenumber equation for infinite Prandtl number with different initial conditions (dots). The middle curve starts at the critical point.

enough for quantitative measurements of the wavenumber. Comparisons with other experiments are not really justified since different selection mechanisms will be in effect. However, the results of Croquette & Pocheau (1984) are less than 10 % smaller than the large P results presented here. Their experiments were performed in a horizontally-homogeneous large-aspect-ratio rectangular cell using fluids with $P = 14$ and 70. The selection mechanisms they investigated were based on the movement of a single dislocation and grain boundaries. Both gave very similar results. Thus for large Prandtl numbers, the selected wavenumber appears to be nearly independent of the selection mechanism. On the other hand, for small P the opposite is true. For instance, there is a very large difference between the boundary of the zigzag instability and axisymmetric convection. The former is not a selection mechanism but the mean flow is the only attribute distinguishing the two. Thus the wavenumber is very sensitive to 'large-scale' flows, which tend to be relatively big for small P. This is shown in figure 3, where the mean flow is plotted for two pairs of (supercritical) Rayleigh and Prandtl numbers, and for subcritical flow. We used $z_0 = \frac{1}{2}$, which produces profiles that are symmetric around the mid-layer. Profiles for other values of z_0 are obtained by adding the right-hand side of (25) to those given. For subcritical Rayleigh numbers, the mean flow is given by a quartic polynomial and is independent of R and P. For supercritical convection, $\overline{u}$ depends strongly on P but its amplitude decreases only slightly with increasing R. At the critical point

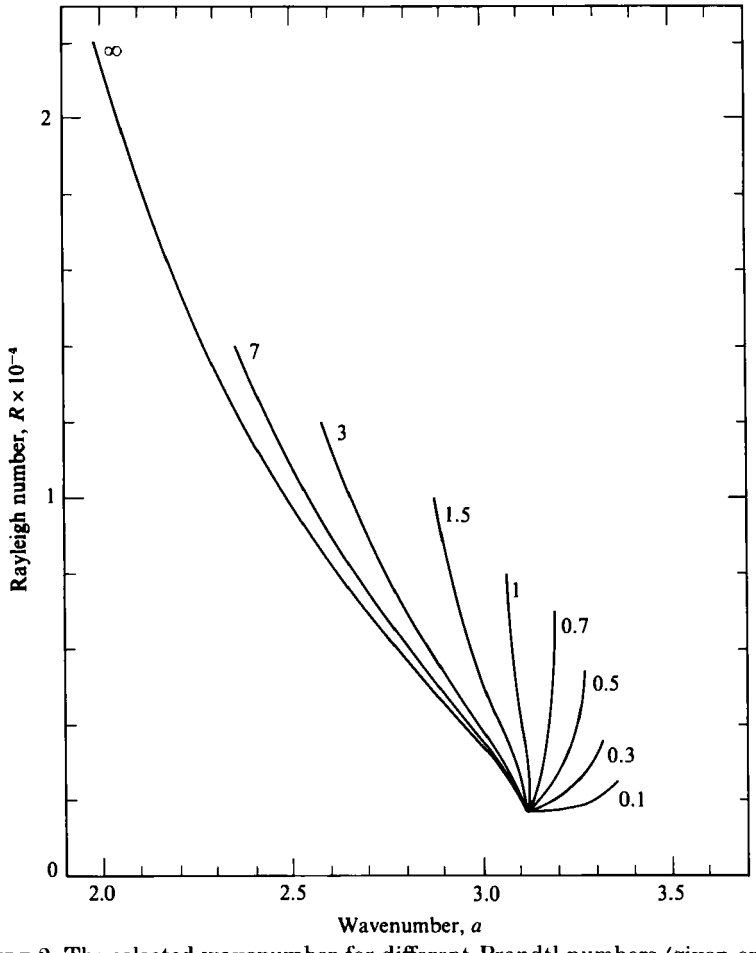

FIGURE 2. The selected wavenumber for different Prandtl numbers (given on curves).

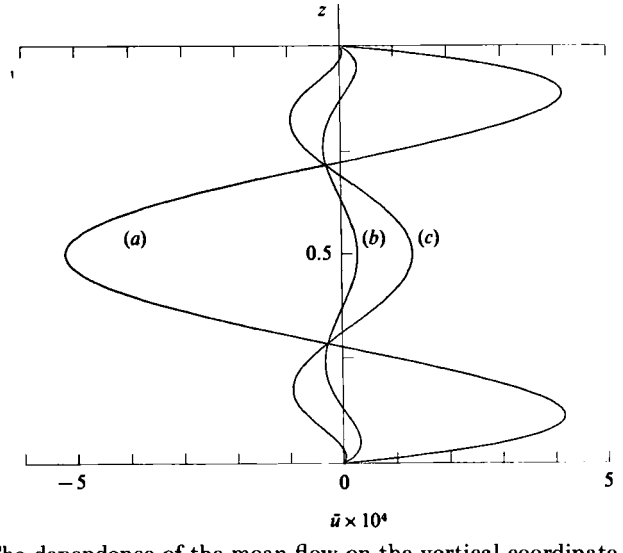

FIGURE 3. The dependence of the mean flow on the vertical coordinate with $z_0 = \frac{1}{2}$ and (*a*) $R < R_c$; (*b*) $R = 7000$, $P = \infty$, $a = 2.696$; (*c*) $R = 2000$, $P = 0.7$, $a = 3.131$.

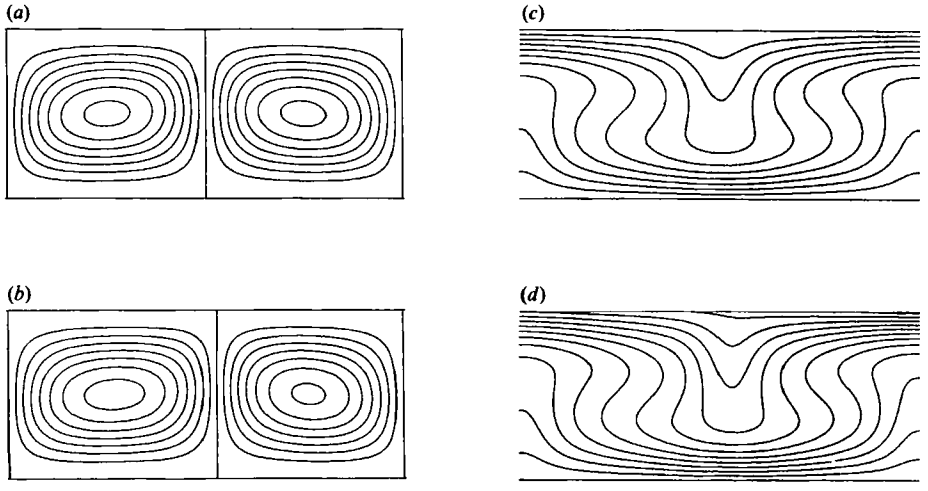

FIGURE 4. Streamlines (a, b), and isotherms (c, d) for $R = 7000$, $P = \infty$ and $z_0 = 0$. The first and third plots are for uniform boundary conditions ($\epsilon = 0$), and the second and fourth for $\epsilon = 0.1$ and $R_0 = 3000$, where ΔT increases to the right. The difference in contour values is 1.0 in (a, b) and 0.1 in (c, d).

the mean flow changes discontinuously with R. This is due directly to the behaviour of $\langle \theta_R \rangle$ at R_c, and is related to the non-uniformity of the expansions at that point.

In figure 4, streamlines (a, b) and isotherms (c, d) are plotted for the case $R = 7000$, $P = \infty$, at the selected wavenumber, $a = 2.696$. Streamlines are defined by contours of

$$\phi_x^{(0)} + \epsilon R_0 \left(\phi_x^{(1)} + \int_0^z \bar{u}(\zeta)\, \mathrm{d}\zeta \right).$$

The first and third plots are for uniform boundary conditions ($\epsilon = 0$), which are to be compared to the second and fourth plots respectively, where $\epsilon = 0.1$, $R_0 = 3000$ and $z_0 = 0$ are assumed. In figure 4 (b) we see that the convection roll that turns with the mean flow (the one on the left) is larger than the other, as expected. However, the strength of this roll is only slightly larger, which is not expected. It turns out that the perturbation field $\boldsymbol{U}^{(1)}$ almost cancels the effect of the mean flow in strengthening the left-hand roll and weakening the right-hand roll, but complements it in increasing the difference in size of the two rolls.

5. Conclusions

We have presented here the derivation of an ordinary differential equation governing wavenumber selection when the temperature boundary conditions are slowly varying in one direction. Solutions were given for Rayleigh numbers up to the vicinity of the point where straight convection rolls become unstable to three-dimensional or time-dependent disturbances, and for several Prandtl numbers. It was found that the selected wavenumber increases monotonically with decreasing P for a given R, and that it increases with R when $P < 0.7$. These trends were also found for axisymmetric convection (Buell & Catton 1986), but are opposite to the ones generally seen in uncontrolled experiments with uniform boundary conditions. This is due to the fact that in the latter case, selection mechanisms different from the one considered here will be in effect, and that these mechanisms are, in general, very sensitive to the Prandtl number (especially when it is $\leqslant O(1)$).

Kramer & Riecke (1985) showed that the selected wavenumber is unique if the temperature ramp connects to a subcritical region. This was assumed implicitly in most of the results when we took the initial condition to be the critical point. Calculations were also performed with other initial conditions to show that even if the convection layer does not contain the critical point, the resulting band of wavenumbers at high Rayleigh numbers will be very small.

The authors acknowledge useful discussions with Professors F. H. Busse, M. C. Cross and R. E. Kelly. Suggestions from the referees also helped to improve the presentation. The research reported here was partly supported by the National Science Foundation under Grant No. MEA 81-05542, and by the Department of Energy for the use of the Cray XMP at the National MFE Computer Center (Lawrence Livermore National Laboratory).

Appendix

We give here the expressions for the elements of the nonlinear vector operator $\mathbf{M}$ and the linear matrix operators L and L^*:

$$\mathbf{M}_1[U] = \frac{\mathrm{d}a}{\mathrm{d}R}\Big[\Big(15\frac{\partial^4}{\partial x^4}+12\frac{\partial^4}{\partial x^2\,\partial z^2}+\frac{\partial^4}{\partial z^4}\Big)\phi_x - R\theta_x - \frac{1}{P}(\phi_{xxz}(3\phi_{xxx}+\phi_{xzz}) + \phi_{xz}(4\phi_{xxzz}+11\phi_{xxxx}) - \phi_{xx}(5\phi_{xxxz}+4\phi_{xzzz}) - \phi_x\nabla^2\phi_{xxz})\Big] + a\Big[\Big(6\frac{\partial^4}{\partial x^4}+8\frac{\partial^4}{\partial x^2\,\partial z^2}+2\frac{\partial^4}{\partial z^4}\Big)\phi_{xR} - 2R\theta_{xR} - 2\theta_x - \frac{1}{P}(\phi_{zR}\nabla^2\phi_{xxx} - 2\phi_{xR}\nabla^2\phi_{xxz} + 2\phi_{xzR}\nabla^2\phi_{xx} - 3\phi_{xxR}\nabla^2\phi_{xz} + \phi_{xz}(5\phi_{xxxxR}+3\phi_{xxzzR}) - \phi_{xx}(4\phi_{xxxzR}+2\phi_{xzzzR}) + \phi_{xxz}(4\phi_{xxxR}+2\phi_{xzzR}) - \phi_{xxx}(3\phi_{xxzR}+\phi_{zzzR}) + \overline{u}\nabla^2\phi_{xxx} - \overline{u}_{zz}\phi_{xxx})\Big], \tag{A 1a}$$

$$\mathbf{M}_2[U] = \frac{\mathrm{d}a}{\mathrm{d}R}[\theta_x - \phi_x + \phi_x\theta_z] + a\Big[2\theta_{xR} - 2\phi_{xR} - \phi_{zR}\theta_x - \phi_{xz}\theta_R + 2\phi_{xR}\theta_z + \frac{2}{R}\theta_x - \frac{1}{R}\phi_{xz}(\theta+z_0-z) - \theta_x\overline{u}\Big], \tag{A 1b}$$

$$\mathsf{L}_{11} = \nabla^4\frac{\partial^2}{\partial x^2} - \frac{1}{P}\Big[\phi^{(0)}_{xz}\nabla^2\frac{\partial^3}{\partial x^3} + \nabla^2\phi^{(0)}_{xxx}\frac{\partial^2}{\partial x\,\partial z} - \phi^{(0)}_{xx}\nabla^2\frac{\partial^3}{\partial x^2\,\partial z} - \nabla^2\phi^{(0)}_{xxz}\frac{\partial^2}{\partial x^2} + \phi^{(0)}_{xxz}\nabla^2\frac{\partial^2}{\partial x^2} + \nabla^2\phi^{(0)}_{xz}\frac{\partial^3}{\partial x^2\,\partial z} - \phi^{(0)}_{xxx}\nabla^2\frac{\partial^2}{\partial x\,\partial z} - \nabla^2\phi^{(0)}_{xz}\frac{\partial^3}{\partial x^3}\Big], \tag{A 2a}$$

$$\mathsf{L}_{12} = -R\frac{\partial^2}{\partial x^2}, \tag{A 2b}$$

$$\mathsf{L}_{21} = -\frac{\partial^2}{\partial x^2} - \theta^{(0)}_x\frac{\partial^2}{\partial x\,\partial z} + \theta^{(0)}_z\frac{\partial^2}{\partial x^2}, \tag{A 2c}$$

$$\mathsf{L}_{22} = \nabla^2 - \phi^{(0)}_{xz}\frac{\partial}{\partial x} + \phi^{(0)}_{xx}\frac{\partial}{\partial z}, \tag{A 2d}$$

$$\mathsf{L}_{11}^{*} = \nabla^4 \frac{\partial^2}{\partial x^2} - \frac{1}{P}\Big[\phi_{xx}^{(0)} \nabla^2 \frac{\partial^3}{\partial x^2 \partial z} - \phi_{xz}^{(0)} \nabla^2 \frac{\partial^3}{\partial x^3} + \phi_{xxz}^{(0)} \Big(\frac{\partial^4}{\partial x^2 \partial z^2} - 3\frac{\partial^4}{\partial x^4}\Big)$$
$$+ (3\phi_{xxx}^{(0)} - 2\phi_{xzz}^{(0)}) \frac{\partial^4}{\partial x^3 \partial z} + \phi_{xxx}^{(0)} \frac{\partial^4}{\partial x \partial z^3} + 2\phi_{xxxz}^{(0)} \Big(\frac{\partial^3}{\partial x \partial z^2} - \frac{\partial^3}{\partial x^3}\Big)$$
$$+ 2(\phi_{xxxx}^{(0)} - \phi_{xxzz}^{(0)}) \frac{\partial^3}{\partial x^2 \partial z}\Big], \tag{A 3a}$$

$$\mathsf{L}_{12}^{*} = -\frac{\partial^2}{\partial x^2} - \theta_x^{(0)} \frac{\partial^2}{\partial x \partial z} + \theta_z^{(0)} \frac{\partial^2}{\partial x^2} + \theta_{xz}^{(0)} \frac{\partial}{\partial x} - \theta_{xx}^{(0)} \frac{\partial}{\partial z}, \tag{A 3b}$$

$$\mathsf{L}_{21}^{*} = -R \frac{\partial^2}{\partial x^2}, \tag{A 3c}$$

$$\mathsf{L}_{22}^{*} = \nabla^2 + \phi_{xz}^{(0)} \frac{\partial}{\partial x} - \phi_{xx}^{(0)} \frac{\partial}{\partial z}. \tag{A 3d}$$

REFERENCES

Buell, J. C. 1986 The operator compact implicit method for fourth order differential equations. *SIAM J. Sci. Stat. Comp.* **7**, 1232–1245.

Buell, J. C. & Catton, I. 1986 Wavenumber selection in large-amplitude axisymmetric convection. *Phys. Fluids* **29**, 23–30.

Busse, F. H. 1967 On the stability of two-dimensional convection in a layer heated from below. *J. Math. Phys.* **46**, 140–150.

Clever, R. M. & Busse, F. H. 1974 Transition to time-dependent convection. *J. Fluid Mech.* **65**, 625–645.

Croquette, V. & Pocheau, A. 1984 Wavenumber selection in Rayleigh–Bénard convective structure. In *Cellular Structures in Instabilities* (ed. J. E. Wesfried & S. Zaleski), pp. 104–126. Springer.

Cross, M. C. & Newell, A. C. 1984 Convection patterns in large aspect ratio systems. *Physica* **10D**, 299–328.

Glansdorff, P. & Prigogine, I. 1971 *Thermodynamic Theory of Structure, Stability, and Fluctuations.* Wiley-Interscience.

Koschmieder, E. L. 1966 On convection on a nonuniformly heated plane. *Beitr. Phys. Atmos.* **39**, 208–216.

Kramer, L., Ben-Jacob, E., Brand, H. & Cross, M. C. 1982 Wavelength selection in systems far from equilibrium. *Phys. Rev. Lett.* **49**, 1891–1894.

Kramer, L. & Riecke, H. 1985 Wavelength selection in Rayleigh–Bénard convection. *Z. Phys.* B**59**, 245–251.

McDonough, J. M. 1980 The Rayleigh–Bénard problem on a horizontally unbounded domain: determination of the wavenumber of convection. Ph.D. dissertation, School of Engineering and Applied Science, University of California, Los Angeles.

McDonough, J. M. & Catton, I. 1982 A mixed finite difference-Galerkin method for two-dimensional convection in a square box. *Intl J. Heat Mass Transfer* **25**, 1137–1146.

Malkus, W. V. R. & Veronis, G. 1958 Finite amplitude cellular convection. *J. Fluid Mech.* **4**, 225–260.

Manneville, P. & Piquemal, J. M. 1983 Zigzag instability and axisymmetric rolls in Rayleigh–Bénard convection: The effects of curvature. *Phys. Rev.* A**28**, 1774–1790.

Meyer-Spasche, R. & Keller, H. B. 1978 *Numerical study of Taylor-vortex flows between rotating cylinders.* Applied Mathematics Report, California Institute of Technology, Pasadena.

Meyer-Spasche, R. & Keller, H. B. 1980 Computations of the axisymmetric flow between rotating cylinders. *J. Comp. Phys.* **35**, 100–109.

Platzman, G. W. 1965 The spectral dynamics of laminar convection. *J. Fluid Mech.* **23**, 481–510.

SRULIJES, J. A. 1979 Zellularkonvection in behalten mit horizontalen temperaturgradienten. Doctoral thesis, Fakultat fur Maschinenbau, Universität Karlsruhe.

STEPLEMAN, R. S. 1976 Tridiagonal fourth order approximations to general two-point nonlinear boundary value problems with mixed boundary conditions. *Math. Comp.* **30**, 92–103.

WALTON, I. C. 1982 On the onset of Rayleigh–Bénard convection in a fluid layer of slowly increasing depth. *Stud. Appl. Maths* **67**, 199–216.

WALTON, I. C. 1983 The onset of cellular convection in a shallow two-dimensional container of fluid heated non-uniformly from below. *J. Fluid Mech.* **131**, 455–470.